scientific reports

Check for updates

OPEN

Caftaric acid attenuates kidney and remote organ damage induced by renal ischemia-reperfusion injury

Fazile Nur Ekinci Akdemir[1], Mustafa Can Güler[2], Ersen Eraslan[3], Ayhan Tanyeli[2]✉ & Serkan Yildirim[4]

Oxidative stress and inflammation are indispensable components of ischemia-reperfusion (IR) injury. In this study, we investigated the effects of low and high doses of caftaric acid (CA) on reducing kidney and remote organ damage induced by IR. We divided Wistar rats into four groups: sham, IR, low (40 mg/kg body weight (BW)), and high (80 mg/kg BW) CA groups. IR (1 h ischemia, 24 h reperfusion) was applied to all groups, except the sham one. Following the experimental period, we removed kidney and lung tissues to assess biochemical, histopathological, and immunohistochemical parameters. In the IR group, oxidant parameters (malondialdehyde (MDA), myeloperoxidase (MPO), total oxidant status (TOS), oxidative stress index (OSI)) increased, and antioxidant level parameters (superoxide dismutase (SOD) and total antioxidant status (TAS)) diminished. In addition, Microtubule-associated protein light chain 3 (LC3), cyclooxygenase-2 (COX-2), and caspase-3 immunopositivity were severe in the IR group. CA treatment improved the LC3, COX-2, and caspase-3 immunopositivity, lowered the oxidant level, and enhanced the antioxidant capacity. Histopathological findings were consistent with the data. In light of all our results, CA is effective against oxidative stress, autophagy, apoptosis, and inflammation in the renal IR experimental model.

Keywords Oxidative stress, Apoptosis, Autophagy, Caftaric acid, Ischemia-reperfusion, Acute kidney injury, Lung

Ischemia-reperfusion (IR) injury is a complex pathological condition that occurs when blood flow and oxygen supply are restored to an organ after diminished circulation. While essential for tissue recovery, this restoration can paradoxically lead to further cellular damage due to a cascade of biochemical events triggered by the sudden influx of oxygen and nutrients. The initial lack of blood flow results in hypoxic tissue damage, exacerbated upon reperfusion due to oxidative stress, inflammation, and apoptosis[1–3]. Excessive reactive oxygen species (ROS) production can induce oxidative stress, inflammatory reactions, and apoptosis[4].

The kidneys are highly vascularized organs that receive significant blood flow, making them particularly susceptible to IR injury. Renal IR may cause acute kidney injury (AKI), a clinical condition with morbidity and mortality[5]. AKI is strongly related to distant organ injury, including lungs[6]. Acute lung injury is a widely extrarenal condition during AKI[7].

During renal IR, excessive ROS formation leads to cellular damage, inflammation, and oxidative stress[8,9]. ROS may harm lipids, proteins, and DNA[10]. ROS-mediated mitochondrial damage induces cellular injury during renal IR[11]. Myeloperoxidase (MPO) and malondialdehyde (MDA) are oxidant parameters, elevating during renal IR and indicating oxidative stress[12].

ROS overproduction results in apoptosis, a programmed cell death[13]. Caspases, particularly caspase 3, are responsible for this process[14]. Along with ROS, the inflammatory reaction prompts the release of proinflammatory cytokines and cell death[15]. ROS induces cyclooxygenase-2 (COX-2) expression involved in inflammation. Autophagy plays a critical role in maintaining cellular homeostasis and supporting cell survival during IR injury[16]. Microtubule-associated protein light chain 3 (LC3) is a highly utilized marker for autophagy[17].

Several studies examined various molecules to support the antioxidant defense as an exogenous agent to reduce the oxidative damage caused by renal IR[18–20]. The multiple plants are an effective source for advancing medical agents[21]. One of the most critical potential active compounds in purple cones, caffeic acid derivatives, is

[1]Department of Nutrition and Dietetics, Faculty of Health Science, Ağrı İbrahim Çeçen University, Ağrı, Turkey. [2]Department of Physiology, Faculty of Medicine, Atatürk University, Erzurum 25240, Turkey. [3]Department of Physiology, Faculty of Medicine, Bandırma OnYedi Eylül University, Balıkesir, Turkey. [4]Department of Pathology, Faculty of Veterinary, Atatürk University, Erzurum, Turkey. ✉email: ayhan.tanyeli@atauni.edu.tr

caftaric acid (CA, Fig. 1), representing biological activities[22]. The medicinal benefits of CA involve antiapoptotic, anticholinesterase, anti-radical, anti-antioxidant, antidiuretic, and genoprotective activities[23–25].

Building upon the demonstrated potential of CA, this study is designed to determine its impacts in the context of IR-induced organ dysfunction. We aim to investigate its role in mitigating oxidative stress, controlling inflammatory responses, and improving apoptosis and autophagy. Through this, we hope to enhance our understanding and potentially guide the development of innovative therapeutic strategies for renal IR.

Materials and methods

Chemical materials

We used a 10% povidone-iodine solution (Batticon; Adeka) for disinfection. We preferred ketamine (Ketalar®, Pfizer, Istanbul) and xylazine hydrochloride (Rompun®, Bayer, Istanbul) for anesthesia. Ketamine/xylazine anesthesia doses (100/15 mg/kg body weight (BW), intraperitoneal (i.p.)) were inspired by another experimental rat model[26]. We purchased CA (purity ≥ 97.0%, CAS Number: 67879-58-7) from Sigma Aldrich (Germany). CA doses were based on previous experimental research[24,27].

Ethical approval

This study was approved by the Experimental Animals Local Ethics Committee of Atatürk University (Date:27.04.2018/Number:100). All methods are reported in accordance with ARRIVE guidelines (https://arriveguidelines.org). All methods were carried out in accordance with relevant guidelines and regulations.

Experimental animals

All animals were obtained from the Experimental Animal Research and Application Center of Atatürk University (ATADEM). Also, animal experiments were carried out in ATADEM. All animals were kept in polypropylene cages under standard laboratory conditions (mean humidity ~ % 55, balanced temperature ~ 22 °C, and controlled 12;12 light-dark). Animals were fed standard laboratory food and tap water. However, the animals were fasted 24 h before the experiment.

Preoperative preparation

The rats were fixed in dorsal anatomical position (Fig. 2a). The back region was shaved (Fig. 2b). Following the disinfection with 10% povidone-iodine solution (Fig. 2c), ketamine/xylazine (was administered for anesthesia (Fig. 2d).

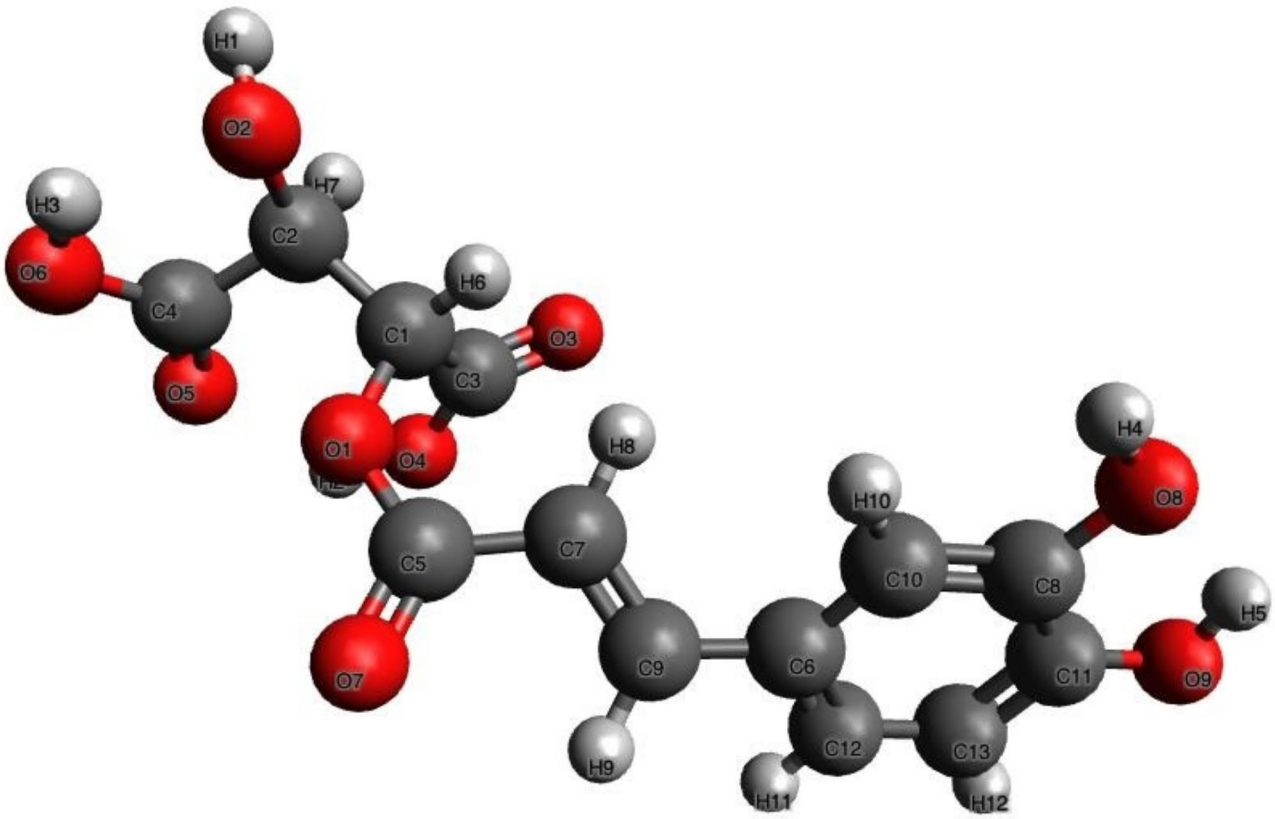

Fig. 1. 3D chemical structure of caftaric acid (Created with Avogadro version 1.2.0., http://avogadro.cc/).

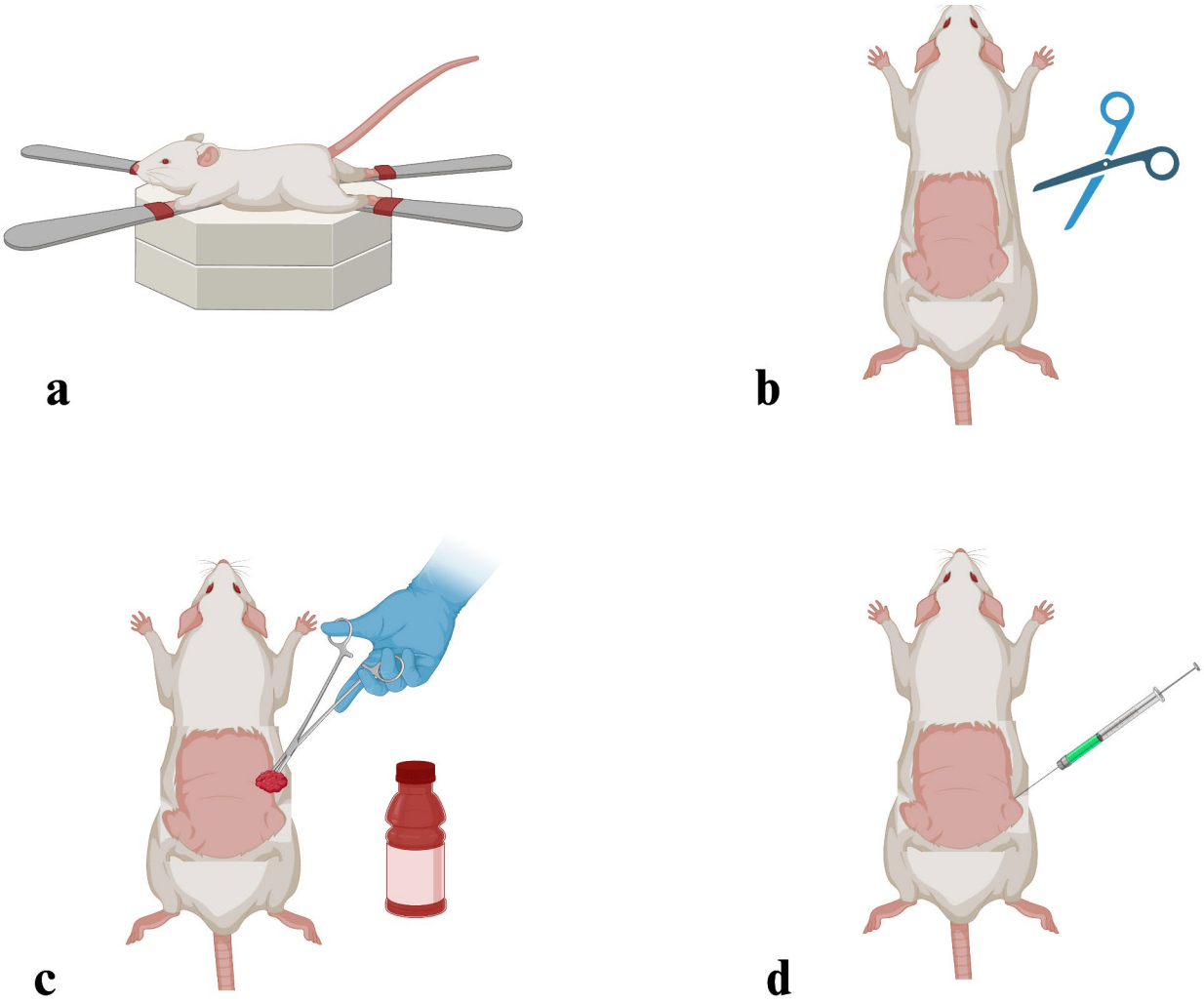

Fig. 2. Representation of the preoperative operation, (**a**) Fixation of the experimental animal in dorsal position, (**b**) Shaving the back region, (**c**) Disinfection of the shaved area, (**d**) Anesthesia administration before the surgical process (Created with BioRender.com).

Groups and experimental design

Weighing 210 ± 10 g, 32 Wistar Albino rats were used and divided into 4 groups (Fig. 3).

Sham Group (n = 8): The back region was opened with an incision and closed again. No additional process was executed (Fig. 3a).

IR Group (n = 8): After the incision, bilateral renal artery blood flow was occluded using steel clamps (Kent Scientific Corporation, USA) for 60 min (ischemia). Then, the blood circulation was released for 24 h (Fig. 3b). This method was selected according to a previous study[28].

Low dose-CA-treated (40 mg/kg CA) Group (n = 8): A 40 mg/kg BW CA dose[29,30] was administered i.p. just before reperfusion, and the IR model was performed as described in the IR group (Fig. 3c).

High dose-CA-treated (80 mg/kg CA) Group (n = 8): An 80 mg/kg BW dose[30] of CA was administered i.p. before the reperfusion and IR model was carried out (Fig. 3d).

With the completion of the reperfusion period, all animals were sacrificed by using a high dose of thiopental sodium (50 mg/kg), as described in previous studies[31,32], and kidney and lung tissue samples were collected. The tissue samples were stored under necessary conditions until biochemical, histopathological, and immunohistochemical analyses.

Biochemical measurements

Determination of superoxide dismutase (SOD) activity, Malondialdehyde (MDA) level, and Myeloperoxidase (MPO) activity is based on previous studies[33–35]. SOD, MPO, and MDA measurements were performed via Thermo Fisher Scientific, USA kits. Total antioxidant status (TAS) and total oxidant status (TOS) values were measured with the commercial kits (Rel Assay Diagnostics, Gaziantep, Turkey). The ratio of TOS to TAS is accepted as the oxidative stress index (OSI)[19].

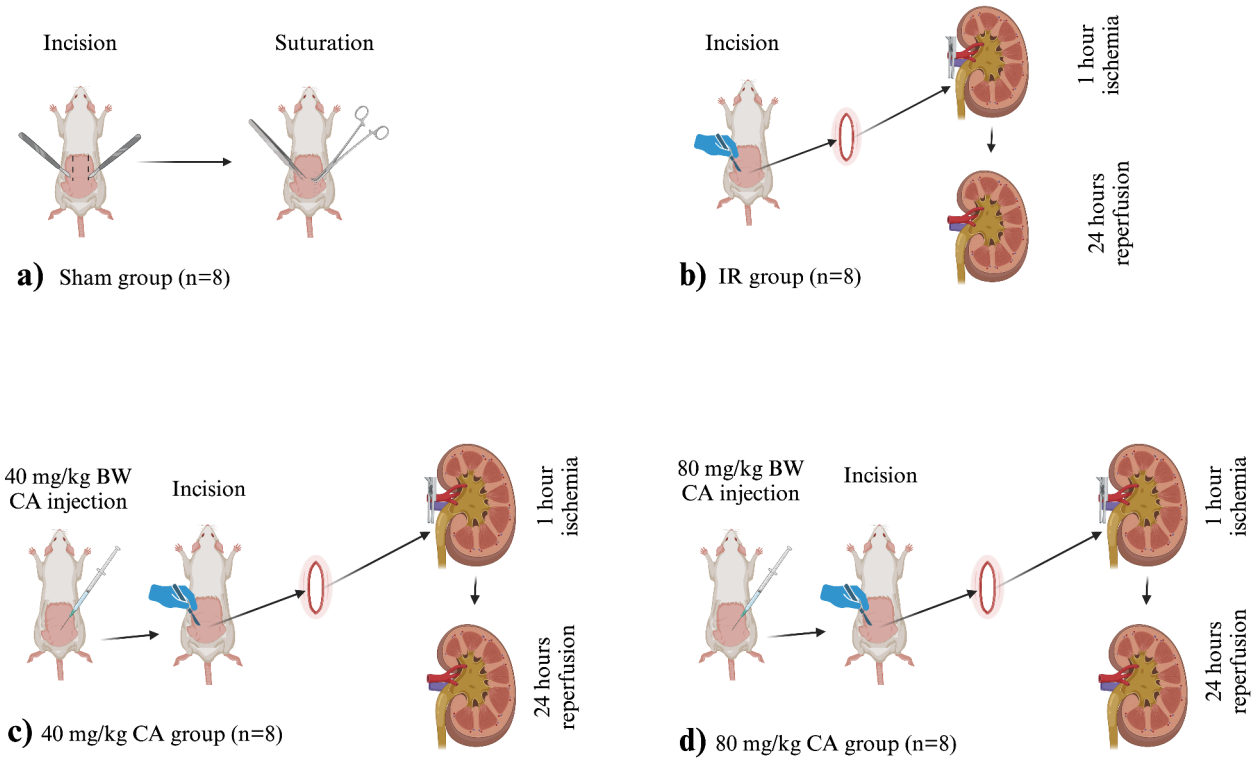

Fig. 3. Experimental design of the renal ischemia reperfusion rat model, (**a**) Sham group, back region incision and suturation, no additional intervention, (**b**) IR group, after the incision, renal arteries and veins were clamped for 60 min, following 24 h reperfusion, (**c**) 40 mg/kg CA group, 40 mg/kg CA was administered i.p. 30 min before the IR process, (**d**) 80 mg/kg CA group, 80 mg/kg CA was administered i.p. 30 min before the IR process. CA = Caftaric acid, IR = Ischemia reperfusion, (Created with BioRender.com).

Immunohistochemical measurements

Upon completion of the experiment, the tissue samples were retained in a 10% neutral formalin solution. Then, tissues were washed in tap water and embedded in paraffin blocks after tissue tracing procedures. After deparaffinization, it was kept in 3% H_2O_2 for 10 min to inactivate endogenous peroxidase activity, and then it was washed in phosphate buffer solution (PBS). The tissues were placed for 10 min at 500W into antigen retrieval solution to remove antigens and washed in PBS. A protein block solution was added to prevent nonspecific binding and washed in PBS. Caspase-3 (Novus Biological, Cat. No. NB600-1235, Dilution: 1/100) as primer anybody, LC3 (Abcam, Cat. No: ab48394 Dilution:1/200) and Cyclooxygenase 2 (COX-2) (Abcam, Cat No: ab15191, Dilution: 1/200) were applied to the sections washed with PBS. Finally, the procedure described by the exposed mouse and rabbit-specific HRP/DAB detection IHC kit (Abcam: ab80436) was followed. 3,3'-diaminobenzidine chromogen was used, and contrast stained with hematoxylin.

Histopathological examinations

At the end of the experiment, the tissue samples were placed in a 10% buffered neutral (pH: 7.2) formalin solution and kept for 48 h for fixation. Then, the tissues underwent histopathological follow-up and were embedded in paraffin. Consecutive thin serial sections of 5 µ thickness were taken from the paraffinized tissues on standard slides. Sections taken from standard slides were stained with hematoxylin and eosin. Histopathological changes in the lungs were examined regarding hyperplasia in the lung tissue and thickening in the interalveolar septum, and changes in the kidney were reviewed in terms of bleeding, necrosis, and hyalinization.

Statistical analyses

All results of our experiments are presented as Mean ± Standard Error Mean (SEM). Firstly, a one-way analysis of variances (ANOVA) was performed, followed by post-hoc testing for inter-group comparisons using the Tukey test. A p-value was accepted as significant at level 0.05. The differences between the groups of obtained data for immunohistochemical results were analyzed by the Kruskal Wallis test and the Mann Whitney U test to detect the groups forming the difference.

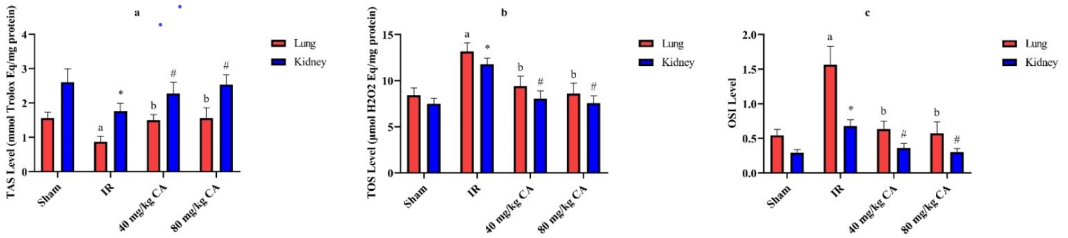

Fig. 4. Effects of CA treatment on oxidative and antioxidative parameters in kidney and lung tissues following IR injury, (**a**) TAS (mmol/L) values of kidney and lung tissues in all groups. (**b**) TOS (µmol/L) values of kidney and lung tissues in all groups. (**c**) OSI values of kidney and lung tissues in all groups. Different letters indicate statistically difference (a = IR group compared to sham group and b = CA groups compared to IR group, $p < 0.05$). * and # represent statistically difference (* = IR group compared to sham group and # = CA groups compared to IR group, $p < 0.05$). TAS = Total antioxidant status, TOS = Total oxidant status, OSI = Oxidative stress index, CA = Caftaric acid, IR = Ischemia reperfusion.

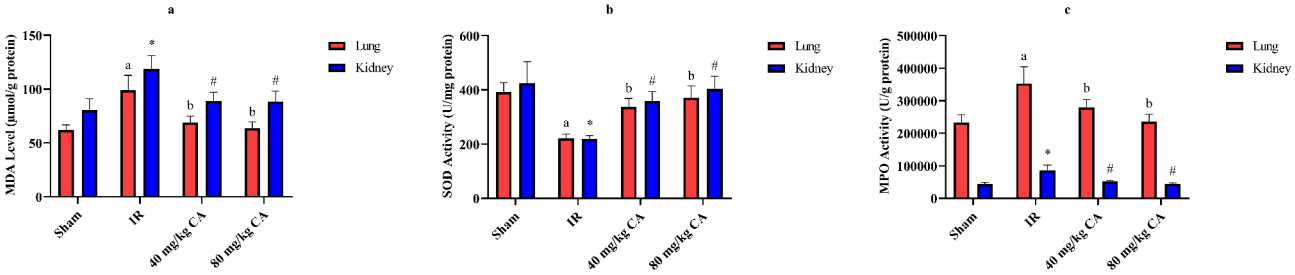

Fig. 5. Effects of CA treatment on oxidative and antioxidative parameters in kidney and lung tissues following IR injury (**a**) MDA (µmol/g protein) values of kidney and lung tissues in all groups. (**b**) SOD (U/g protein) values of kidney and lung tissues in all groups. **c)** MPO (U/g protein) values of kidney and lung tissues in all groups. Different letters indicate statistically difference (a = IR group compared to sham group and b = CA groups compared to IR group $p < 0.05$). * and # represent statistically difference (* = IR group compared to sham group and # = CA groups compared to IR group, $p < 0.05$). MPO = Myeloperoxidase, MDA = Malondialdehyde, SOD = Superoxide dismutase, CA = Caftaric acid, IR = Ischemia reperfusion.

Results

Biochemical results

CA treatment enhanced this antioxidant enzyme activity. TOS and OSI levels were significantly increased in the kidney and lung tissues of the IR group when compared to sham and CA treatment groups (Figs. 4b and c). In contrast, TAS diminished in the IR group (see Fig. 4a). TAS elevated due to low (40 mg/kg BW) and high (80 mg/kg BW) doses of CA treatment.

MDA level and MPO activity increased in the IR group (Fig. 5a and c). MDA concentration and MPO activity declined in the CA treatment groups compared to the IR group (Fig. 5a and c). However, high and low doses of CA groups showed no significant difference, compared to each other.

SOD enzyme activity was significantly reduced in the IR group compared to the sham group (Fig. 5b). CA treatment greatly improved SOD activity compared to the IR group. Still, there was no significant difference between the high and low doses of CA groups.

Immunohistochemical results of the renal tissue

Caspase-3 immunopositivity was not observed in the sham group (Fig. 6a) and high dose CA group (Fig. 6d) but was detected in the tubular epithelial cells, and glomerulus of the IR group as most intense (Fig. 6b). In the low dose CA group, caspase-3 immunopositivity diminished in tubular epithelial cells and inflammatory cells in the intertubular area (Fig. 6c).

LC3 immunopositivity was not seen in the sham group (Fig. 7a). There was intense LC3 immunoreactivity in the tubular epithelial cells and glomerulus of the IR and low dose of CA groups (Fig. 7b and c). On the other hand, LC3 immunopositivity decreased in tubular epithelial cells and inflammatory cells in the intertubular area of the low dose of CA group (Fig. 7c). High dose of CA treatment improved LC3 immunopositivity and created mild immunoreactivity in the epithelial cells forming Bowman capsule and in the inflammatory cells of the intertubular area (Fig. 7d).

COX-2 immunopositivity was negative in the sham group (Fig. 8a) but positive in the IR and low dose of CA groups' tubular epithelial cells and glomerulus as most intense (Fig. 8b and c). Interestingly, low dose of CA decreased the COX-2 immunopositivity in the tubular epithelial cells and inflammatory cells of the intertubular

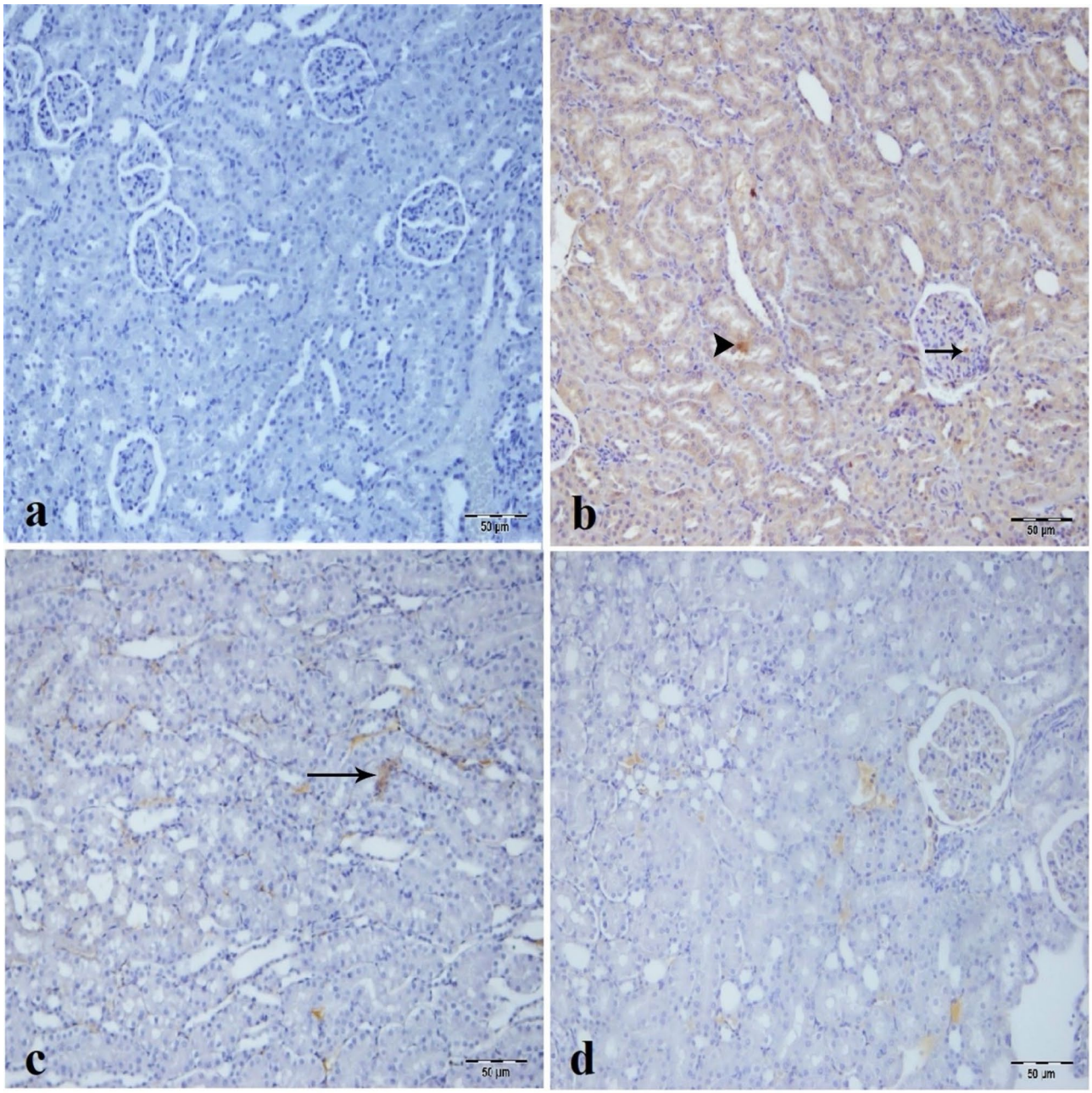

Fig. 6. Immunohistochemical analysis of caspase-3 expression in kidney tissues across experimental groups, (**a**) Sham group. (**b**) IR group, intensive caspase-3 immunopositivity in tubule epithelium (arrowhead) and glomerular structure (arrow) of kidney tissue. (**c**) Low dose of (CA) (40 mg/kg) group mild caspase-3 immunopositivity in inflammatory cells in intertubular area (arrow) of kidney tissue. (**d**) High dose of CA (80 mg/kg) group, nonspecific staining. CA = Caftaric acid.

area (Fig. 8c). The high dose CA group demonstrated a very mild LC3 immunopositivity in tubular epithelial cells and glomerular structure (Fig. 8d).

Immunohistochemical results of the lung tissue

Sham group did not reveal a caspase-3 immunopositivity (Fig. 9a). There was a caspase-3 immunopositivity in inflammatory cells of the peribronchial tissue and interalveolar area of the IR group (Fig. 9b). CA treatment groups improved caspase-3 immunopositivity in the inflammatory cells of the peribronchial tissue and the cells of the interalveolar region (Fig. 9c, d).

Immunohistochemical staining for autophagic cell death did not reveal any LC3 immunopositivity in the sham group (Fig. 10a). IR and low dose of CA groups exhibited intense LC3 immunopositivity in inflammatory cells in the peribronchial tissue and interalveolar area (Fig. 10b and c). In the high dose of the CA group, LC3 immunopositivity decreased in inflammatory cells of the peribronchial tissue (Fig. 10d).

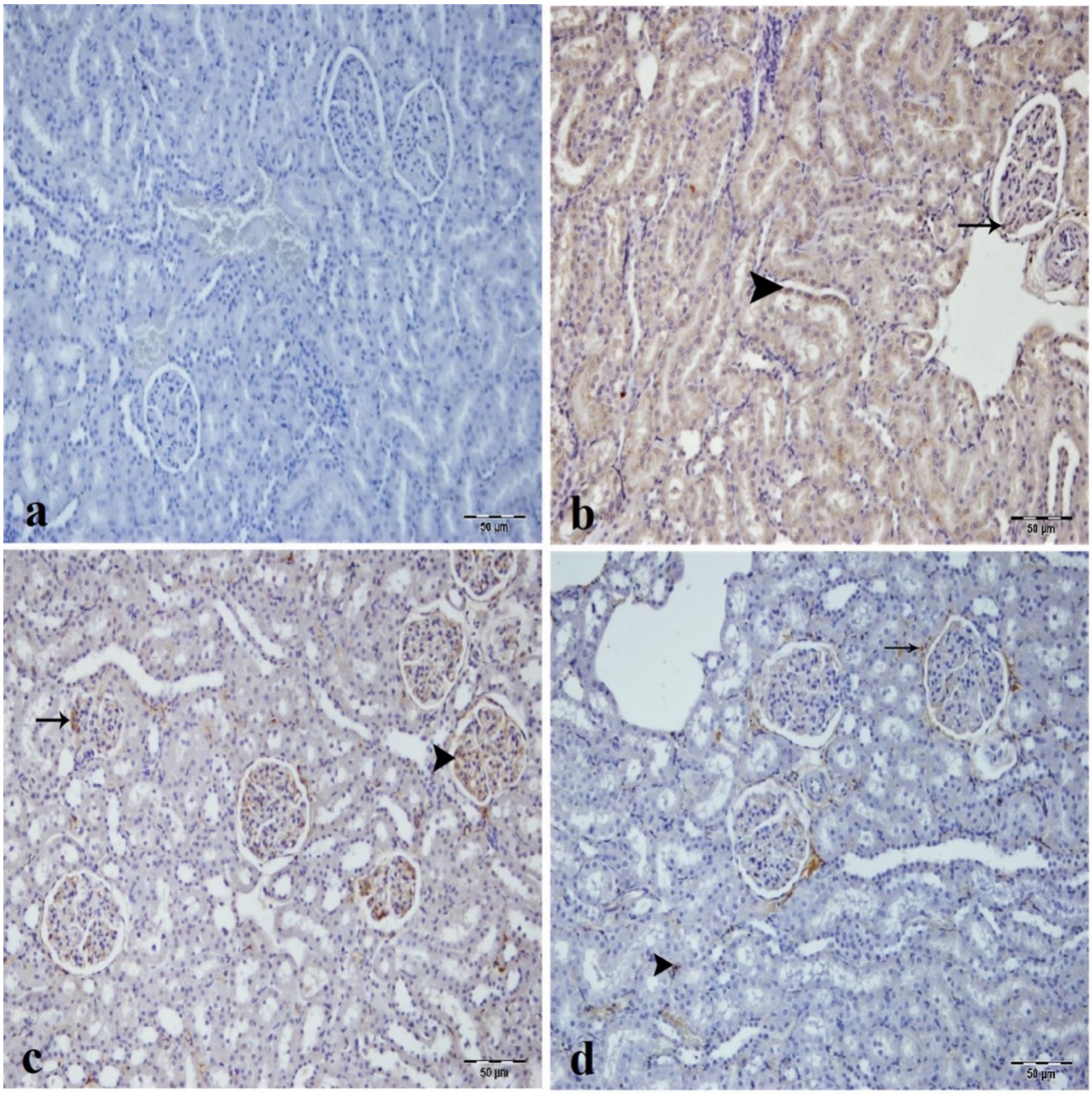

Fig. 7. Immunohistochemical analysis of LC3 expression in kidney tissues across experimental groups, (**a**) Sham group. (**b**) IR group, intensive LC3 immunopositivity in epithelium of tubule (arrowhead) and glomerulus (arrow) of kidney tissue. (**c**) Low dose of CA (40 mg/kg) group, intense LC3 immunopositivity in tubule epithelial cells (arrow) and glomerulus (arrowhead) of kidney tissue. (**d**) High dose of CA (80 mg/kg) group, mild LC3 immunopositivity in tubule epithelial cells (arrowhead) and epithelial portion of bowman capsule (arrow) of kidney tissue. CA = Caftaric acid, IR = Ischemia reperfusion.

COX-2 immunopositivity was not found in the sham group (Fig. 11a). The most intense immunopositivity for COX-2 was in the peribronchial cells of lymphoid tissue in the IR group (Fig. 11b). In low dose of CA group, COX-2 immunopositivity declined in the inflammatory cells of peribronchial tissue (Fig. 11c). The mildest COX-2 immunopositivity was observed in the high dose CA group (Fig. 11d).

Histopathological results of kidney and lung tissue

In general, the renal parenchymal and stromal regions had a normal histological appearance in the sham group (Fig. 12a). Severe tissue damage was detected in the kidney tissues of the IR group (Fig. 12b). This damage was mainly in the form of congestion, bleeding, necrotic tubular, and hyalinization. Still, necrotic changes decreased in the low dose of the CA group (Fig. 12c). Mild bleeding and necrotic changes were observed in the high-dose CA group (Fig. 12d).

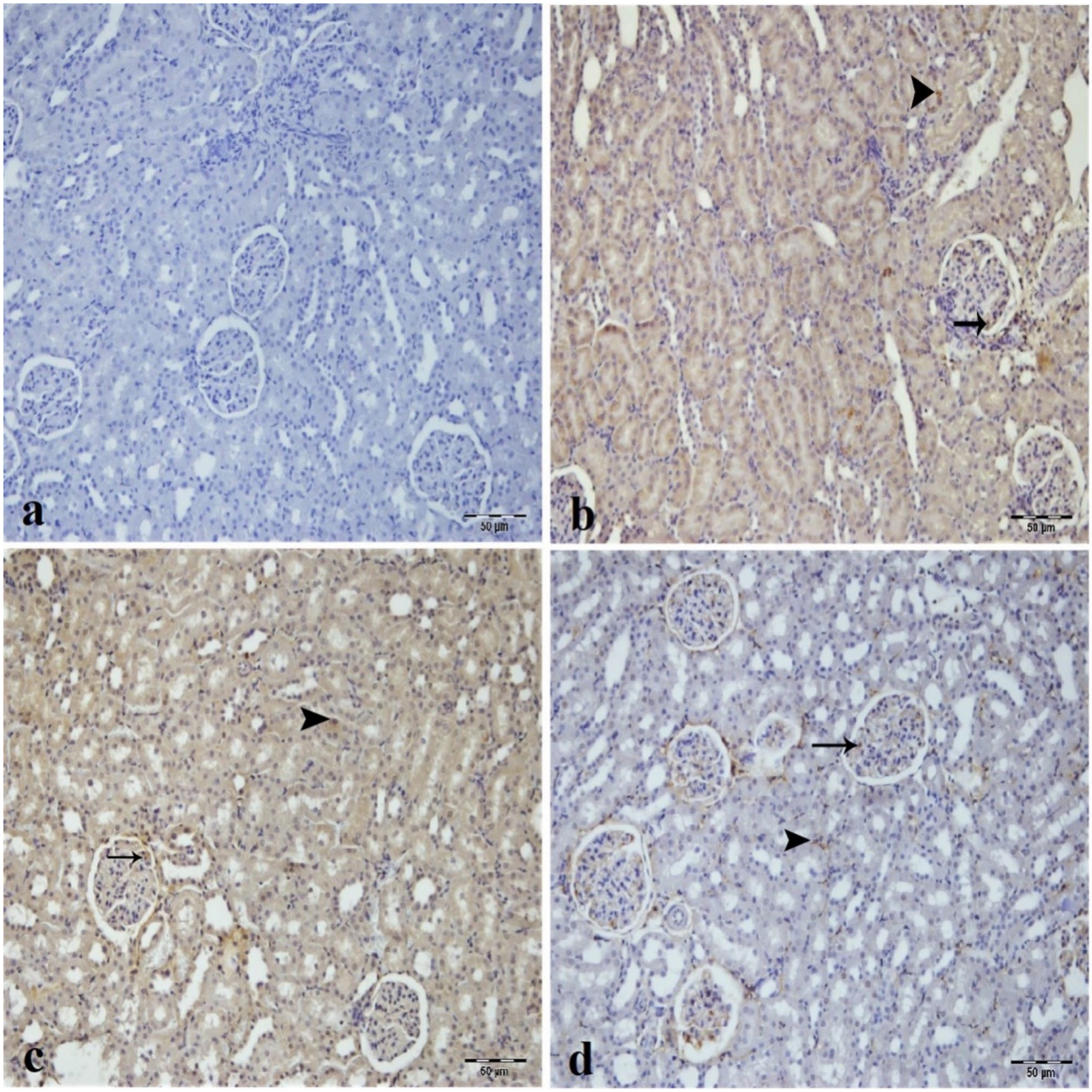

Fig. 8. Immunohistochemical analysis of COX2 expression in kidney tissues across experimental groups, (**a**) Sham group. (**b**) IR group, intensive COX2 immunopositivity in epithelium of tubule (arrowhead) and glomerulus (arrow) of kidney tissue. (**c**) Low dose of CA (40 mg/kg) group, intense COX2 immunopositivity in tubule epithelial cells (arrowhead) and glomerulus (arrow) of kidney tissue. (**d**) High dose of CA (80 mg/kg) group, mild COX2 immunopositivity in tubule epithelial cells (arrowhead) and mild COX2 immunopositivity in glomerular structure of kidney tissue. CA = Caftaric acid, IR = Ischemia reperfusion.

In the histopathological examination of the lung tissue, the alveolar parenchyma had a normal histological appearance in the sham group (Fig. 13a). There was a severe lung tissue hyperplasia in the lung tissues of the IR group (Fig. 13b). Additionally, thickening was detected in the interalveolar area. Although lung hyperplasia decreased in the low-dose CA group, the thickening in the interalveolar area was similar to the IR group (Fig. 13c). Lung tissue hyperplasia decreased, and the interalveolar septum appeared slightly thickened in the high-dose CA group (Fig. 13d).

Discussion

This study demonstrated that CA treatment, at both low (40 mg/kg) and high (80 mg/kg) doses, effectively mitigated renal and lung damage caused by IR injury. CA administration significantly reduced oxidative

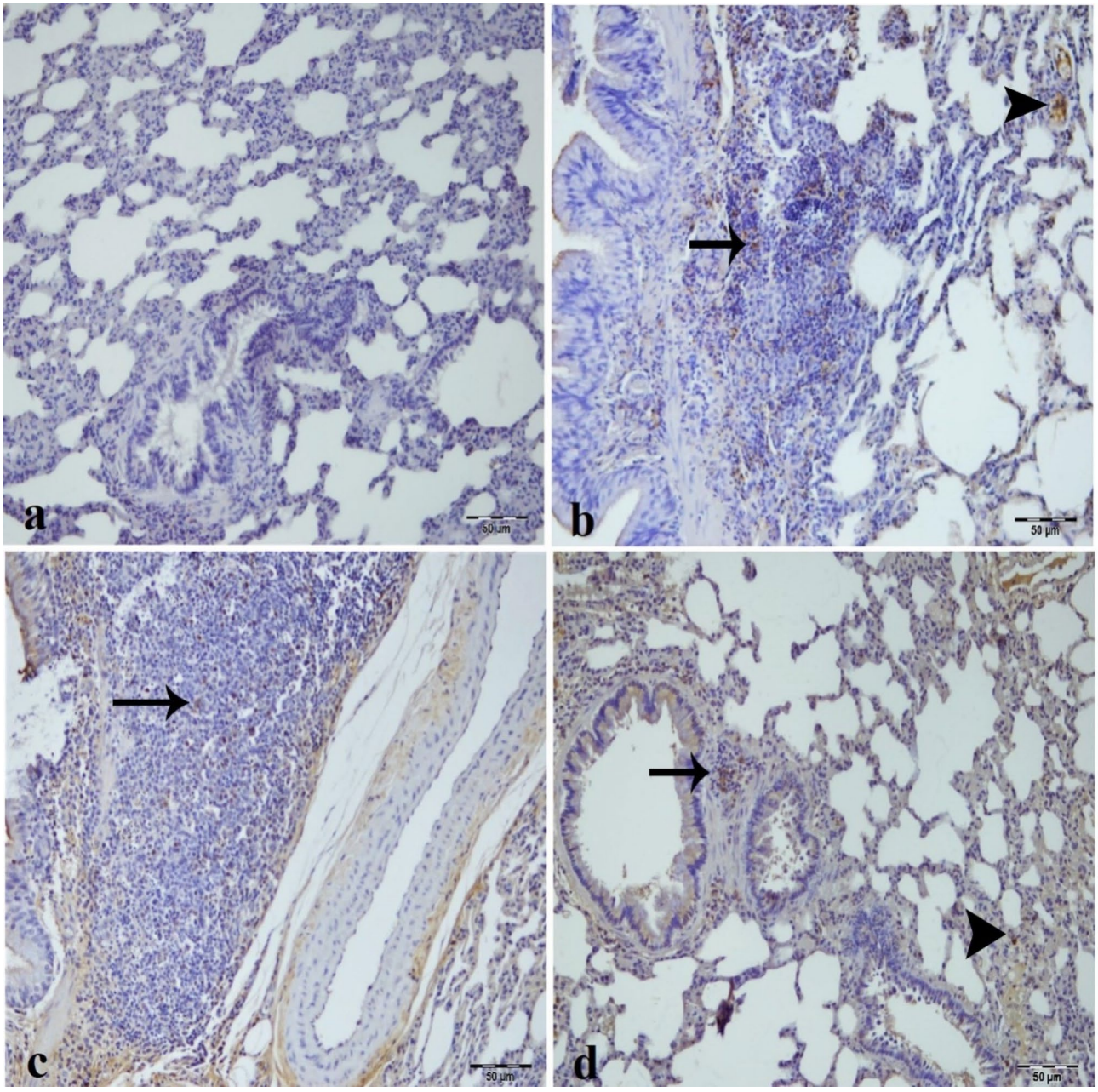

Fig. 9. Immunohistochemical analysis of caspase-3 expression in lung tissues across experimental groups, (**a**) Sham group. (**b**) IR group, intensive caspase-3 immunopositivity in interalveolar area (arrowhead) and inflammatory cells in peribronchial tissue (arrow). (**c**) low dose of CA (40 mg/kg) group, moderate-intensity caspase-3 in inflammatory cells in the peribronchial tissue. (**d**) High dose of CA (80 mg/kg) group, mild caspase-3 immunopositivity in interalveolar area (arrowhead) and inflammatory cells (arrow) in peribronchial tissue. CA = Caftaric acid, IR = Ischemia reperfusion.

stress markers (MDA, MPO, TOS, OSI) and increased antioxidant levels (SOD, TAS) in kidney and lung tissues. Immunohistochemical analysis revealed diminished caspase-3, COX-2, and LC3 immunopositivity with CA treatment, particularly at higher doses, indicating reduced apoptosis, inflammation, and autophagy. Histopathological findings supported these biochemical results.

In the evolving field of renal research, renal IR injury has garnered significant attention due to its role in AKI and subsequent systemic complications. Renal IR injury is characterized by oxidative stress, inflammation, and cellular apoptosis, leading to renal dysfunction. CA has been widely examined for its potent antioxidant and anti-inflammatory properties. Its efficacy in reducing oxidative stress and inflammation has been demonstrated[36]. Similarly, renal IR injury, characterized by oxidative damage and tissue inflammation, presents a critical challenge in AKI[37]. What remains novel in this context is the investigation of CA as a therapeutic intervention for renal IR injury.

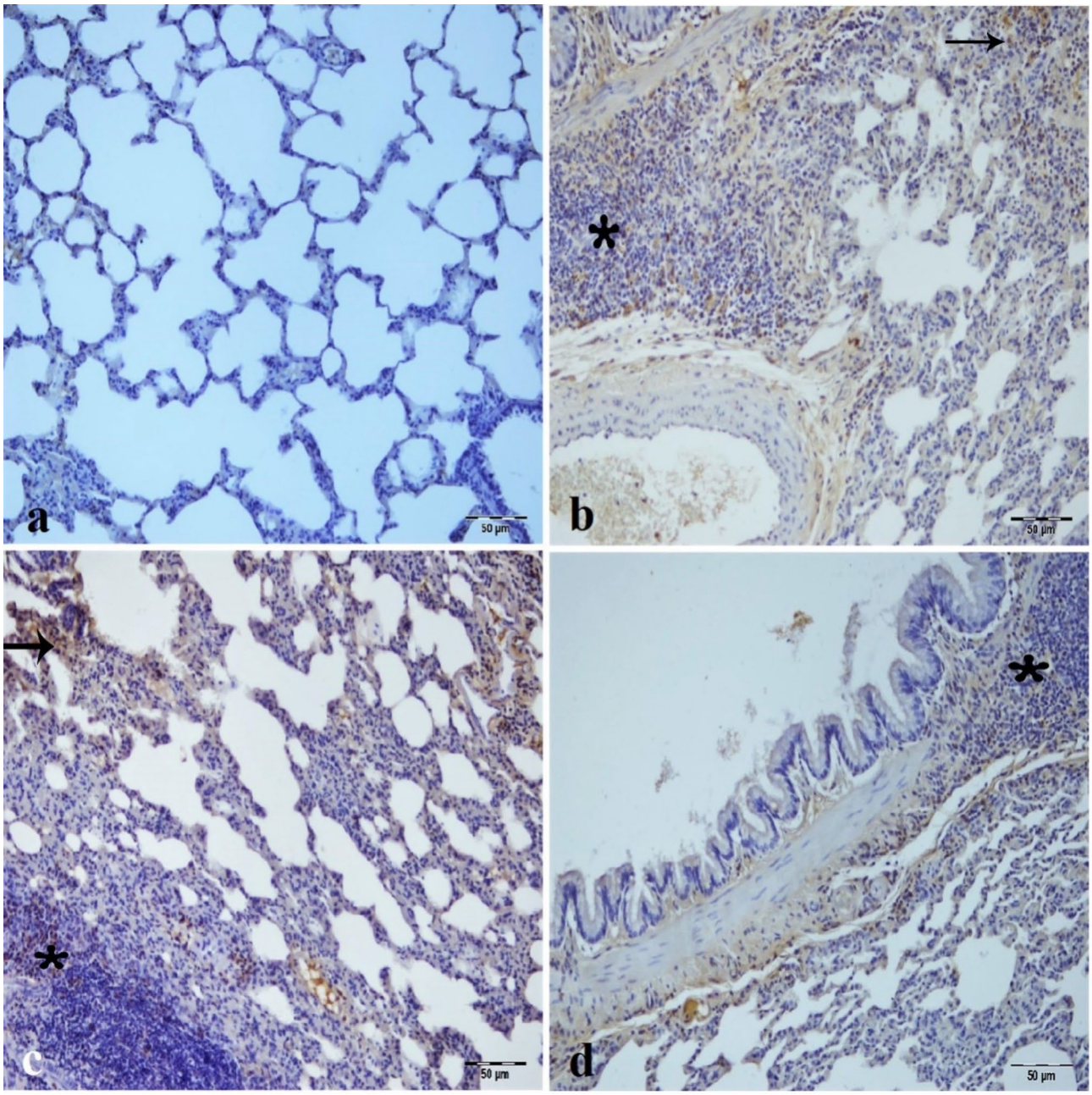

Fig. 10. Immunohistochemical analysis of LC3 expression in lung tissues across experimental groups, (**a**) Sham group. (**b**) IR group, intensive LC3 immunopositivity in interalveolar area (arrow) and inflammatory cells in peribronchial tissue (star). (**c**) Low dose of CA (40 mg/kg) group, moderate-intensity LC3 in inflammatory cells in the peribronchial tissue (star). (**d**) High dose of CA (80 mg/kg) group, mild LC3 immunopositivity in inflammatory cells (star) in peribronchial tissue. CA = Caftaric acid, IR = Ischemia reperfusion.

We conducted this study to estimate the lung as a remote organ, assess the renoprotective effects of different doses of CA in an experimental model of kidney IR, and determine whether the antioxidative, antiapoptotic, and antiautophagic effects were closely associated with kidney and lung protection by CA. The results indicated that the low and high doses of CA attenuated the IR-induced renal and lung injury. Histopathological results substantiated these findings. Besides, Immunopositivity was mild for caspase-3, LC3, and COX-2 at high doses of CA. The more protective effect of the higher dose of CA is limited to its antiapoptotic and anti-inflammatory effects. These results suggest that CA may maintain the physiological structure of lung and renal tissue by reducing oxidative stress, autophagic responses, and apoptotic responses during the IR process.

Renal IR damage is a common cause of AKI. IR damage concerns oxidative stress, apoptosis, autophagy, and renal inflammation[19,38]. Oxidative stress has been known for a long time to play an essential role in the pathophysiology of cancer, aging, obesity, and cardiovascular diseases[39,40]. ROS are products of normal

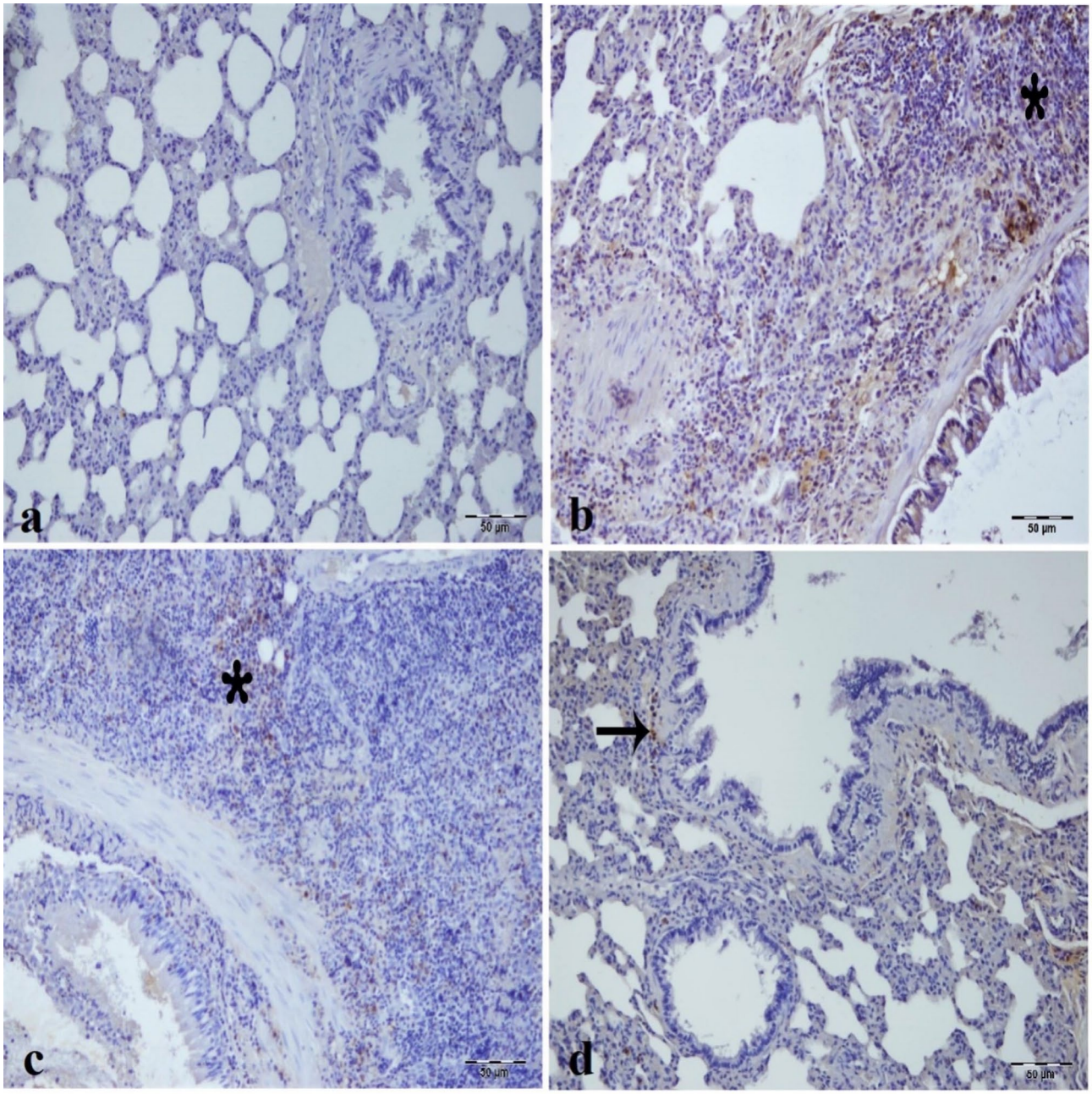

Fig. 11. Immunohistochemical analysis of COX2 expression in lung tissues across experimental groups, (**a**) Sham group. **b**) IR group, intensive COX2 immunopositivity in inflammatory cells in peribronchial tissue (star). (**c**) Low dose of CA (40 mg/kg) group, mild COX2 in inflammatory cells in the peribronchial tissue (star). (**d**) High dose of CA (80 mg/kg) group, mild COX2 immunopositivity in inflammatory cells (arrow) in peribronchial tissue. CA = Caftaric acid, IR = Ischemia reperfusion.

physiologic metabolism in cells, but their excessive production seriously threatens cellular homeostasis and leads to oxidative tissue damage[41,42]. ROS-generating chemical reactions are catalyzed by enzymes such as COX, MPO, and peroxidases[43]. As an inflammatory parameter, MPO can be used to measure the oxidative stress level[44]. COX is the rate-limiting enzyme in converting arachidonic acid to prostaglandin and thromboxane. COX-2 is directly associated with inflammation and is stimulated by many pro-inflammatory markers, including ROS and cytokines. COX-2 is an inducible enzyme overexpressed in human and animal cancer types[43,45]. COX-2 expression is strongly related to various types of I/R injuries via exacerbating inflammation[43,46,47]. The current study showed that COX-2 expression and MPO activity were high in renal and lung tissues due to renal IR. Conversely, CA treatment attenuated COX-2 expression and MPO activity. In addition, the high dose of CA was more effective.

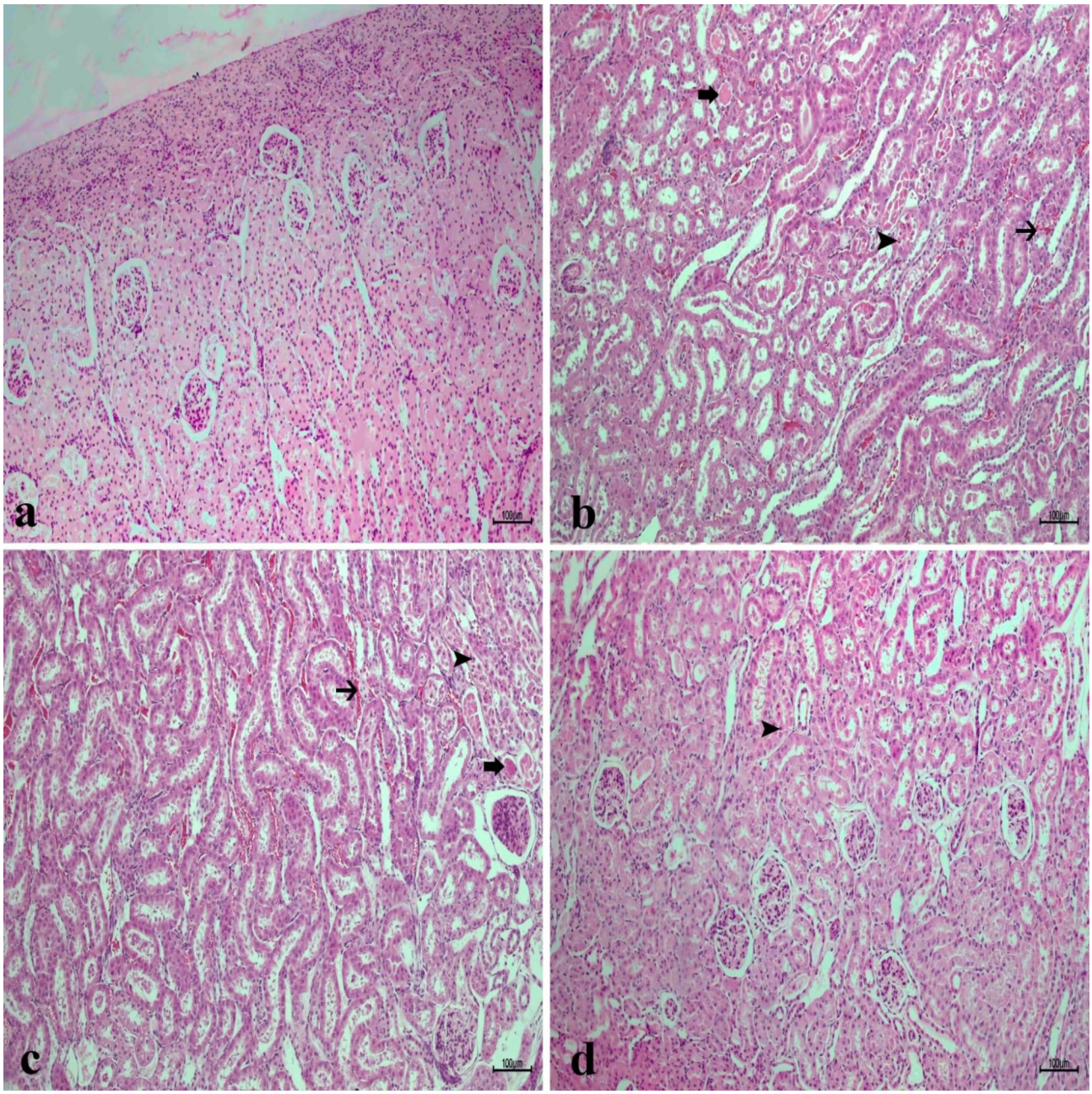

Fig. 12. Histopathological analysis of kidney tissues in experimental groups, (**a**) Sham group (**b**) IR group, necrosis (arrowhead) in the tubule epithelium and bleeding in the intertubular area (thin arrow) and hyalinization in the tubules (thick arrow) (**c**) Low dose of CA (40 mg/kg) group, moderate necrosis in the tubule epithelium (arrowhead) and bleeding in the intertubular area (thin arrow) and hyalinization in the tubules (thick arrow) (**d**) high dose of CA (80 mg/kg) group, mild necrosis in tubular epithelium (arrowhead), H&Ex10. CA = Caftaric acid, IR = Ischemia reperfusion.

TOS measurement is a precision indicator of lipid peroxidation and oxidative stress[20]. SOD and TAS protect tissues from IR-induced oxidative damage by scavenging the ROS. The TOS/TAS ratio is called OSI, an oxidative stress level index[48,49]. In this study, we determined whether the two doses of CA protect the kidney and lung tissues suffering IR injury by inhibiting oxidative stress. Here, the renal IR injury experimental model investigated the change of SOD activities, TAS, TOS, OSI, and MDA levels in the kidney and lung tissues of all groups. MDA, TOS, and OSI elevated, and SOD activity and TAS declined in kidney and lung tissues.

The apoptotic balance between cell viability and death determines the cell's fate. This shifting balance between cell death and pro-cell viability signaling elicits apoptotic consequences in different physiological and pathological conditions[50,51]. Also, apoptosis is an essential physiologic and pathologic mechanism in acute kidney injury renal IR-induced[52]. Apoptotic cell death is the most well-known of the caspase-mediated apoptosis pathways. Moreover, apoptosis is the first mechanism of cell death during renal IR injury[53]. A family of cysteine

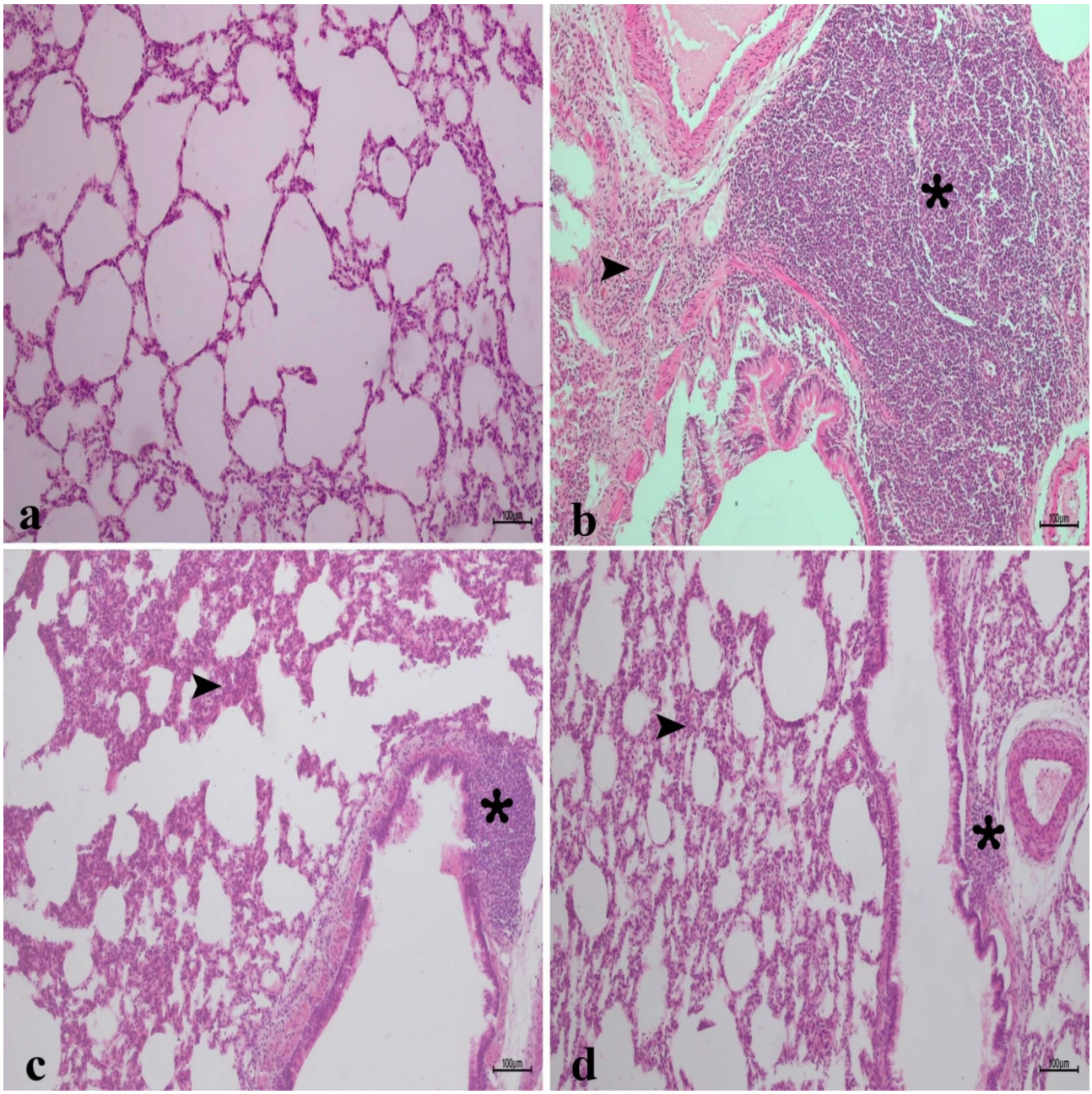

Fig. 13. Histopathological analysis of lung tissues in experimental groups, (**a**) Sham group (**b**) IR group, intense hyperplasia (asterix) in the lung tissue and thickening in the interalveolar area (arrowhead) (**c**) low dose 40 mg/kg CA group, interalveolar thickening of the area (arrowhead) and a decrease in hyperplasia of the lung tissue (asterix). (**d**) High dose 80 mg/kg CA group, slight thickening of the interalveolar area (arrowhead) and a decrease in hyperplasia of the lung tissue (asterix), H&Ex10. CA = Caftaric acid, IR = Ischemia reperfusion.

proteases carries out this process called caspases[54]. Caspase-3, a biomarker identifying cellular apoptosis, is one of the most important apoptotic pathways[55]. Some studies represented caspase-3 expression at severe levels in renal IR injury[56,57]. In our study, we exposed the expression of caspase-3 as a pro-apoptotic protein. We found that the expression level caspase-3 was high in renal IR injury, and the expression of caspase-3 attenuated owing to different doses of CA. Just as apoptotic mechanisms affect the prognosis of autophagy, the autophagy process also involves the prognosis of apoptosis. Autophagy is primarily considered a pro-survival mechanism for the cell and is triggered in response to various stimuli that threaten homeostasis[58].

Autophagy and apoptosis are interlocked in extensive cross-talk[59]. Autophagy exerts a renoprotective effect in models of acute kidney injury (AKI), with its pathways presenting promising targets for therapeutic intervention. Enhanced autophagy in renal IR injury appears to act as a compensatory mechanism to mitigate the damaging consequences of IR injury and the progression to AKI[60]. The ratio of LC3 I to LC3 II is closely associated with the

extent of autophagosome formation, so LC3 II was thought to be an indicator of autophagic activity[61]. Studies have shown that cerebral IR injury triggers autophagic activity by increasing the expression of LC3[62]. Similar to a previous study[63], our results showed that LC3 expression indicated that autophagy was enhanced in kidney and lung tissues induced by renal IR. The lower expression of LC3 was seen due to treatments with CA. The reduction in LC3 levels following CA treatment is not a direct effect of the compound itself but rather a result of diminished autophagic demand due to the improvement of metabolic disturbances post-CA administration.

Conclusion

In the direction of all our findings, this study would be the first to indicate that two doses of CA protect kidney and lung tissues against IR-induced renal injury. Possible physiopathological mechanisms include alleviating oxidative stress/apoptosis/autophagy and modulating the TOS/TAS level with caspase-3, COX-2, and LC3 expressions.

Data availability

The datasets used and analyzed during the current study are available from the corresponding author upon reasonable request.

Received: 25 September 2024; Accepted: 10 December 2024
Published online: 28 December 2024

References

1. Turner, C. T. et al. Sulfaphenazole reduces thermal and pressure injury severity through rapid restoration of tissue perfusion. *Sci. Rep.* **12**, 12622. https://doi.org/10.1038/s41598-022-16512-9 (2022).
2. Heusch, G. Myocardial ischaemia–reperfusion injury and cardioprotection in perspective. *Nat. Rev. Cardiol.* **17**, 773–789. https://doi.org/10.1038/s41569-020-0403-y (2020).
3. Mu, Q. et al. Ligustrazine nanoparticle hitchhiking on neutrophils for enhanced therapy of cerebral ischemia-reperfusion injury. *Adv. Sci.* **10**, 2301348. https://doi.org/10.1002/advs.202301348 (2023).
4. Ko, S. H. et al. Effect of high-dose vitamin C on renal ischemia-reperfusion injury. *Biomed. Pharmacother.* **173**, 116407. https://doi.org/10.1016/j.biopha.2024.116407 (2024).
5. Lima-Posada, I. et al. Gender differences in the acute kidney injury to chronic kidney disease transition. *Sci. Rep.* **7**, 12270. https://doi.org/10.1038/s41598-017-09630-2 (2017).
6. Lee, S. A., Cozzi, M., Bush, E. L. & Rabb, H. Distant organ dysfunction in acute kidney injury: A review. *Am. J. Kidney Dis.* **72**, 846–856. https://doi.org/10.1053/j.ajkd.2018.03.028 (2018).
7. Basu, R. K. & Wheeler, D. S. Kidney–lung cross-talk and acute kidney injury. *Pediatr. Nephrol.* **28**, 2239–2248. https://doi.org/10.1007/s00467-012-2386-3 (2013).
8. Bayoumi, A. A., Ahmad, E. A., Ibrahim, I. A. A. E. H., Mahmoud, M. F. & Elbatreek, M. H. Inhibition of both NOX and TNF-α exerts substantial renoprotective effects in renal ischemia reperfusion injury rat model. *Eur. J. Pharmacol.* **970**, 176507. https://doi.org/10.1016/j.ejphar.2024.176507 (2024).
9. Liu, S. et al. Trehalose attenuates renal ischemia-reperfusion injury by enhancing autophagy and inhibiting oxidative stress and inflammation. *Am. J. Physiol. Renal. Physiol.* **318**, F994-f1005. https://doi.org/10.1152/ajprenal.00568.2019 (2020).
10. Xia, K. et al. Degradation of histone deacetylase 6 alleviates ROS-mediated apoptosis in renal ischemia-reperfusion injury. *Biomedicine & Pharmacotherapy* **165**, 115128. https://doi.org/10.1016/j.biopha.2023.115128 (2023).
11. Granata, S. et al. Oxidative stress and ischemia/reperfusion injury in kidney transplantation: Focus on ferroptosis, mitophagy and new antioxidants. *Antioxidants (Basel)* **11**. https://doi.org/10.3390/antiox11040769 (2022).
12. Güler, M. C., Akpinar, E., Tanyeli, A., Çomakli, S. & Bayir, Y. Costunolide prevents renal ischemia-reperfusion injury in rats by reducing autophagy, apoptosis, inflammation, and DNA damage. *Iran. J. Basic Med. Sci.* **26**, 1168–1176. https://doi.org/10.22038/ijbms.2023.71779.15596 (2023).
13. Wang, J. et al. Osthole induces apoptosis and caspase-3/GSDME-dependent pyroptosis via NQO1-mediated ROS generation in HeLa cells. *Oxid. Med. Cell. Longev.* **2022**, 8585598. https://doi.org/10.1155/2022/8585598 (2022).
14. Zhao, R.-M. et al. ROS-responsive bola-lipid nanoparticles as a codelivery system for gene/photodynamic combination therapy. *Mol. Pharm.* **21**, 2012–2024. https://doi.org/10.1021/acs.molpharmaceut.4c00053 (2024).
15. Jang, H. R. & Rabb, H. Immune cells in experimental acute kidney injury. *Nat. Rev. Nephrol.* **11**, 88–101. https://doi.org/10.1038/nrneph.2014.180 (2015).
16. Yang, J. et al. Melatonin pretreatment alleviates renal ischemia-reperfusion injury by promoting autophagic flux via TLR4/MyD88/MEK/ERK/mTORC1 signaling. *FASEB J.* **34**, 12324–12337. https://doi.org/10.1096/fj.202001252R (2020).
17. Feng, S., Ji, J., Li, H. & Zhang, X. H2S alleviates renal ischemia and reperfusion injury by suppressing ERS-induced autophagy. *Transplant. Immunol.* **83**, 102006. https://doi.org/10.1016/j.trim.2024.102006 (2024).
18. Güler, M. C. et al. Higenamine decreased oxidative kidney damage induced by ischemia reperfusion in rats. *Kafkas Univ. Vet. Fak.* **26**, 365–370. https://doi.org/10.9775/kvfd.2019.23250 (2020).
19. Tanyeli, A., Guler, M. C., Eraslan, E. & Ekinci Akdemir, F. N. Barbaloin attenuates ischemia reperfusion-induced oxidative renal injury via antioxidant and antiinflammatory effects. *Med. Sci.* **9**, 246–250 (2020).
20. Topdağı, Ö. et al. Preventive effects of fraxin on ischemia/reperfusion-induced acute kidney injury in rats. *Life Sci.* **242**, 117217. https://doi.org/10.1016/j.lfs.2019.117217 (2020).
21. Tajner-Czopek, A. et al. Study of antioxidant activity of some medicinal plants having high content of caffeic acid derivatives. *Antioxidants* **9** (2020).
22. Saima, et al. Caftaric acid ameliorates oxidative stress, inflammation, and bladder overactivity in rats having interstitial cystitis: An in silico study. *ACS Omega* **8**, 28196–28206. https://doi.org/10.1021/acsomega.3c01450 (2023).
23. Tanyeli, A., Akdemir, F. N. E., Eraslan, E., Güler, M. C. & Nacar, T. Anti-oxidant and anti-inflamatuar effectiveness of caftaric acid on gastric ulcer induced by indomethacin in rats. *Gen. Physiol. Biophys.* **38**, 175–181 (2019).
24. Koriem, K. M. M. & Arbid, M. S. Role of caftaric acid in lead-associated nephrotoxicity in rats via antidiuretic, antioxidant and anti-apoptotic activities. *J. Complement. Integr. Med.* **15**. https://doi.org/10.1515/jcim-2017-0024 (2017).
25. Boulebd, H., Mechler, A., Hoa, N. T. & Vo, Q. V. Insights on the kinetics and mechanisms of the peroxyl radical scavenging capacity of caftaric acid: The important role of the acid-base equilibrium. *New J. Chem.* **46**, 7403–7409. https://doi.org/10.1039/d2nj00377e (2022).
26. Güler, M. C. et al. Alleviating sepsis: Revealing the protective role of costunolide in a cecal ligation and puncture rat model. *Iran. J. Basic Med. Sci.* **27**, 567–576. https://doi.org/10.22038/ijbms.2024.75372.16335 (2024).

27. Ekinci Akdemir, F. N. & Tanyeli, A. The effect of Fraxin against lung and testis damage induced by testicular torsion/detorsion in rats. *Ann. Med. Res.* **27**, 2769–2774 (2020).
28. Topdağı, Ö. et al. Preventive effects of fraxin on ischemia/reperfusion-induced acute kidney injury in rats. *Life Sci.* **242**, 117217. https://doi.org/10.1016/j.lfs.2019.117217 (2020).
29. Koriem, K. M. & Soliman, R. E. Chlorogenic and caftaric acids in liver toxicity and oxidative stress induced by methamphetamine. *J. Toxicol.* **2014**, 583494. https://doi.org/10.1155/2014/583494 (2014).
30. Tanyeli, A., Ekinci Akdemir, F. N., Eraslan, E., Güler, M. C. & Nacar, T. Anti-oxidant and anti-inflamatuar effectiveness of caftaric acid on gastric ulcer induced by indomethacin in rats. *Gen. Physiol. Biophys.* **38**, 175–181. https://doi.org/10.4149/gpb_2018035 (2019).
31. Ferah Okkay, I. et al. Bromelain protects against cisplatin-induced ocular toxicity through mitigating oxidative stress and inflammation. *Drug Chem. Toxicol.* **46**, 69–76. https://doi.org/10.1080/01480545.2021.2011308 (2023).
32. Gezer, A., Ustundag, H., Mendil, A. S., Bedir, G. & Duysak, L. Hepatoprotective effects of resveratrol on α-amanitin-induced liver toxicity in rats. *Toxicon* **247**, 107855. https://doi.org/10.1016/j.toxicon.2024.107855 (2024).
33. Sun, Y., Oberley, L. W. & Li, Y. A simple method for clinical assay of superoxide-dismutase. *Clin. Chem.* **34**, 497–500 (1988).
34. Ohkawa, H., Ohishi, N. & Yagi, K. Assay for lipid peroxides in animal-tissues by thiobarbituric acid reaction. *Anal. Biochem.* **95**, 351–358. https://doi.org/10.1016/0003-2697(79)90738-3 (1979).
35. Bradley, P. P., Priebat, D. A., Christensen, R. D. & Rothstein, G. Measurement of cutaneous inflammation—estimation of neutrophil content with an enzyme marker. *J. Invest. Dermatol.* **78**, 206–209. https://doi.org/10.1111/1523-1747.ep12506462 (1982).
36. Ahmadi, F., Samadi, A., Sepehr, E., Rahimi, A. & Shabala, S. Increasing medicinal and phytochemical compounds of coneflower (Echinacea purpurea L.) as affected by NO3−/NH4+ ratio and perlite particle size in hydroponics. *Sci. Rep.* **11**, 15202. https://doi.org/10.1038/s41598-021-94589-4 (2021).
37. Last, J. et al. MFG-E8-derived peptide attenuates inflammation and injury after renal ischemia-reperfusion in mice. *Heliyon* **6**. https://doi.org/10.1016/j.heliyon.2020.e05794 (2020).
38. Malek, M. & Nematbakhsh, M. Renal ischemia/reperfusion injury; from pathophysiology to treatment. *J. Renal. Inj. Prev.* **4**, 20–27. https://doi.org/10.12861/jrip.2015.06 (2015).
39. Si, C. et al. Association of total and different food-derived advanced glycation end-products with risks of all-cause and cause-specific mortality. *Food Funct.* **15**, 1553–1561. https://doi.org/10.1039/D3FO03945E (2024).
40. Hajam, Y. A. et al. Oxidative stress in human pathology and aging: Molecular mechanisms and perspectives. *Cells* **11** (2022).
41. Gutmann, C., Siow, R., Gwozdz, A. M., Saha, P. & Smith, A. Reactive oxygen species in venous thrombosis. *Int. J. Mol. Sci.* **21** (2020).
42. Checa, J. & Aran, J. M. Reactive oxygen species: Drivers of physiological and pathological processes. *J. Inflamm. Res.* **13**, 1057–1073. https://doi.org/10.2147/jir.S275595 (2020).
43. Tóth, S. et al. Quercetin attenuates the ischemia reperfusion induced COX-2 and MPO expression in the small intestine mucosa. *Biomed. Pharmacother.* **95**, 346–354. https://doi.org/10.1016/j.biopha.2017.08.038 (2017).
44. Cosic-Mujkanovic, N. et al. myeloperoxidase alters lung cancer cell function to benefit their survival. *Antioxidants* **12** (2023).
45. Uchida, K. HNE as an inducer of COX-2. *Free Radic. Bio. Med.* **111**, 169–172. https://doi.org/10.1016/j.freeradbiomed.2017.02.004 (2017).
46. Li, M. & Zheng, Z. Protective effect of parecoxib sodium against ischemia reperfusion-induced intestinal injury. *Mol. Med. Rep.* **24**, 776. https://doi.org/10.3892/mmr.2021.12416 (2021).
47. Li, Y. et al. Maternal inflammation exaggerates offspring susceptibility to cerebral ischemia-reperfusion injury via the COX-2/PGD2/DP2 pathway activation. *Oxid. Med. Cell. Longev.* **2022**, 1571705. https://doi.org/10.1155/2022/1571705 (2022).
48. Topdagi Yilmaz, E. A. et al. The therapeutic effect of naringin on ovarian and lung damages created by adnexal torsion/detorsion: A biochemical study. *Ann. Med. Res.* **27**, 2438–2442 (2020).
49. Tanyeli, A. et al. Barbaloin attenuates ischemia reperfusion-induced oxidative renal injury via antioxidant and anti-inflammatory effects. *Med. Sci.* **9**, 246–250 (2020).
50. Stella, S. et al. Glucose-dependent effect of insulin receptor isoforms on tamoxifen antitumor activity in estrogen receptor-positive breast cancer cells. *Front. Endocrinol.* **14** (2023).
51. Anson, F., Thayumanavan, S. & Hardy, J. A. Exogenous introduction of initiator and executioner caspases results in different apoptotic outcomes. *JACS Au* **1**, 1240–1256. https://doi.org/10.1021/jacsau.1c00261 (2021).
52. Xu, Y. et al. Nanoparticle—mediated dual delivery of resveratrol and DAP5 ameliorates kidney ischemia/reperfusion injury by inhibiting cell apoptosis and inflammation. *Oncotarget* **8**, 39547–39558. https://doi.org/10.18632/oncotarget.17135 (2017).
53. Qian, Z. et al. ROS-responsive MSC-derived exosome mimetics carrying MHY1485 alleviate renal ischemia reperfusion injury through multiple mechanisms. *ACS Omega* **9**, 24853–24863. https://doi.org/10.1021/acsomega.4c01624 (2024).
54. Jung, W. et al. Expression of caspases in the pig endometrium throughout the estrous cycle and at the maternal-conceptus interface during pregnancy and regulation by steroid hormones and cytokines. *Front. Vet. Sci.* **8** (2021).
55. Asadi, M. et al. Caspase-3: Structure, function, and biotechnological aspects. *Biotechnol. Appl. Bioc.* **69**, 1633–1645. https://doi.org/10.1002/bab.2233 (2022).
56. Tan, X. H. et al. Fibroblast growth factor 2 protects against renal ischaemia/reperfusion injury by attenuating mitochondrial damage and proinflammatory signalling. *J. Cell. Mol. Med.* **21**, 2909–2925. https://doi.org/10.1111/jcmm.13203 (2017).
57. Li, Y. J. et al. Propofol prevents renal ischemia-reperfusion injury via inhibiting the oxidative stress pathways. *Cell. Physiol. Biochem.* **37**, 14–26. https://doi.org/10.1159/000430329 (2015).
58. Tsapras, P. & Nezis, I. P. Caspase involvement in autophagy. *Cell. Death Differ.* **24**, 1369–1379. https://doi.org/10.1038/cdd.2017.43 (2017).
59. Booth, L. A., Tavallai, S., Hamed, H. A., Cruickshanks, N. & Dent, P. The role of cell signalling in the crosstalk between autophagy and apoptosis. *Cell Signal.* **26**, 549–555. https://doi.org/10.1016/j.cellsig.2013.11.028 (2014).
60. Kaushal, G. P. & Shah, S. V. Autophagy in acute kidney injury. *Kidney Int.* **89**, 779–791. https://doi.org/10.1016/j.kint.2015.11.021 (2016).
61. Yang, H. et al. Gelsolin inhibits autophagy by regulating actin depolymerization in pancreatic ductal epithelial cells in acute pancreatitis. *Braz. J. Med. Biol. Res.* **56**, e12279. https://doi.org/10.1590/1414-431X2023e12279 (2023).
62. Luo, J. et al. Platonin protects against cerebral ischemia/reperfusion injury in rats by inhibiting NLRP3 inflammasomes via BNIP3/LC3 signaling mediated autophagy. *Brain Res. Bull.* **180**, 12–23. https://doi.org/10.1016/j.brainresbull.2021.12.008 (2022).
63. Zhang, Y. L., Qiao, S. K., Wang, R. Y. & Guo, X. N. NGAL attenuates renal ischemia/reperfusion injury through autophagy activation and apoptosis inhibition in rats. *Chem.-Biol. Interact.* **289**, 40–46. https://doi.org/10.1016/j.cbi.2018.04.018 (2018).

Acknowledgements

This study was presented as a poster presentation at the 49th Congress of the Turkish Society of Physiological Sciences.

Author contributions

Study design: F.N.E.A., A.T., E.E., M.C.G. Data collection: F.N.E.A., A.T., M.C.G., S.Ç. Data analysis: F.N.E.A.,

A.T., M.C.G., E.E., S.Ç. Supervision: F.N.E.A. Writing of the original paper: F.N.E.A. Revision of the original paper: F.N.E.A., A.T., E. E., M.C.G. Approval of the paper: all authors.

Funding
The author(s) received no financial support for the research, authorship, and/or publication of this article.

Declarations

Competing interests
The authors declare no competing interests.

Additional information
Supplementary Information The online version contains supplementary material available at https://doi.org/10.1038/s41598-024-82912-8.

Correspondence and requests for materials should be addressed to A.T.

Reprints and permissions information is available at www.nature.com/reprints.

Publisher's note Springer Nature remains neutral with regard to jurisdictional claims in published maps and institutional affiliations.